Fiber-Chirped Grating Fabry–Perot Sensor with Multiple-Wavelength-Addressable Free-Spectral Ranges

K. P. Koo, *Member, IEEE,* M. LeBlanc, T. E. Tsai, and S. T. Vohra

***Abstract*— We report the demonstration of a fiber-chirped grating Fabry–Perot (FP) sensor with large dynamic range and high resolution surpassing that of a conventional FP sensor. The chirped grating FP sensor functions as an array of collocated FP cavities with different wavelength addressable cavity lengths or free-spectral ranges. This sensor design allows large dynamic range and high resolution to be achieved in a single compact sensor head. Free-spectral range from 0.04 to 1.3 nm has been achieved. Using this device as a strain sensor, unambiguous (without fringe counting) strain measurements from 3 ± 1 μStrain (limited by probe source resolution) to 1300 μStrain have been measured.**

***Index Terms*— Chirp gratings, Fabry–Perot resonators, fiber-optics, sensors, WDM.**

SHORT-FIBER Fabry–Perot (FP) cavities have been demonstrated as quasi-point sensors for temperature and strain measurements [1], [2]. These single cavity sensors have fixed free-spectral ranges (FSR's) determined by the fixed cavity lengths of the FP cavities. Since the wavelength resolution (the smallest detectable wavelength shift) of a FP cavity is proportional to the product of the cavity finesse and the FSR, a conventional FP sensor with a fixed cavity length and a fixed finesse (determined by the reflectivity of the cavity reflectors) has a predetermined wavelength resolution. In short, large FSR can only be obtained at the expense of a lower wavelength resolution. In sensor applications, small resolvable wavelength shift (high resolution) translates to high sensitivity and large FSR translates to large dynamic range. Both high resolution and large dynamic range are features essential to sensor applications. We propose here a chirped grating FP sensor that provides a single compact sensor head with large dynamic range and high-resolution capabilities beyond that of a conventional (single cavity) FP sensor. In essence, this chirped grating FP sensor functions as an array of collocated FP cavities with different wavelength addressable FSR. This type of sensor can be interrogated easily, for example, by a simple source wavelength scanning scheme.

Manuscript received January 29, 1998; revised March 13, 1998.

K. P. Koo and M. LeBlanc are with the Naval Research Laboratory, Washington DC 20375 USA. They are also with SFA, Inc., Largo, MD 20774 USA.

T. E. Tsai is with the Naval Research Laboratory, Washington DC 20375 USA. He is also with the Virginia Polytechnic Institute, Blacksburg, VA 24061 USA.

S. T. Vohra is with the Naval Research Laboratory, Washington DC 20375 USA.

Publisher Item Identifier S 1041-1135(98)04708-9.

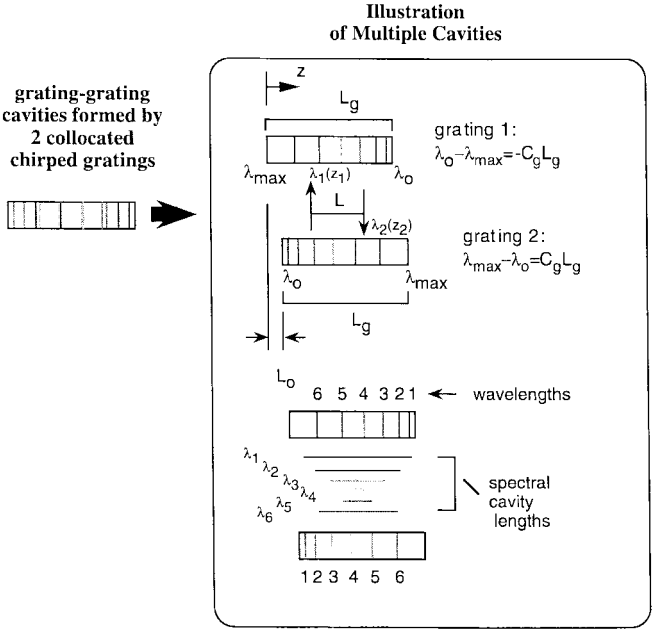

Fig. 1. Illustration of a chirped fiber grating FP sensor with wavelength dependent cavity lengths.

The proposed FP sensor is made up of two collocated fiber chirped gratings arranged such that their chirped direction is opposite to each other. This chirped grating cavity configuration forms multiple spectral (wavelength dependent) FP cavities with different cavity lengths as illustrated in Fig. 1. Note that if the chirped directions of the two gratings are the same, the multiple FP cavities will have equal cavity lengths or FSR's as reported [3]. By interrogating the sensor at a different wavelength band, different spectral FP cavities with different resolution and dynamic range can be addressed.

Using this type of fiber-chirped grating cavity device as a strain sensor, strain on the sensor induces a shift in the FP resonance wavelength of a particular FP cavity which in turn may cause a shift of the operation from one FP cavity to a neighboring FP cavity with a different cavity length. However, it can be shown that for cavity lengths (L_c) less than or equal to the chirped grating length (L_g), the strain can be approximated by the simple expression similar to that for a FP cavity

$$\varepsilon = \frac{1}{\zeta}\,\frac{\Delta\lambda}{\lambda}, \qquad \text{for } L_c \le L_g. \tag{1}$$

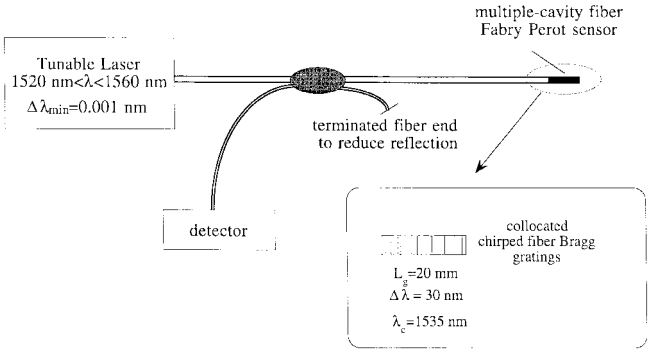

Fig. 2. Experimental setup of a chirped fiber grating FP sensor.

Equation (1) indicates that the strain (ε) on the chirped grating FP cavity can be determined by measuring the change in the resonance wavelength $(\Delta\lambda)$ at the probing wavelength λ with the photo-elastic constant of glass $\zeta = 0.8$. Because of space, details of the derivation of (1) will be presented elsewhere.

Fig. 2 shows a schematic of the chirped grating FP cavity sensor system. A wavelength tunable laser at 1500 nm (Photonetic Tunics 1500) coupled through a 3-dB fiber coupler was used to probe the spectral response of the reflected light from the chirped grating FP cavity sensor at the return port of the fiber coupler. All unused fiber ends were properly terminated to suppress the formation of spurious cavities that can introduce interference signals. The wavelength encoded FP cavity was formed by two collocated in-fiber chirped Bragg grating reflectors with opposite chirped orientation. In-fiber chirped gratings were written by the phase mask technique (exposing a length of hydrogenated fiber with a UV laser at 248 nm through a grating phase mask). Determined by the phase mask, each chirped grating has a wavelength dispersion of $\Delta\lambda_g = 30$ nm centered at 1535 nm over a grating length of $L_g = 2$ cm. The grating reflectivity is ≈50% (calculated from the measured effective finesse of the FP cavity). Further work is needed to determined if higher finesse can be obtained with this type of chirped grating cavity by optimizing the fabrication process. With this chirped grating cavity configuration, there are multiple specific resonant wavelengths corresponding to multiple specific cavity lengths. For perfectly collocated chirped gratings, the largest free spectral range or the shortest cavity length $L_{\min}$ is associated with an interrogation wavelength at the center of the passband of the grating. The smallest FSR or the longest cavity length $L_{\max}$ is associated with interrogation wavelengths near the edges of the passband of the grating. Because the cavity-forming gratings have opposite wavelength chirped orientations, there is a reflection symmetry in the spectral response of the grating cavity as shown in Fig. 3. (If the two gratings were not perfectly collocated, there would be a shift in the interrogation wavelength from the grating centered wavelength corresponding to the shortest cavity length.) As a result of the reflection symmetry in the spectral response, there are two interrogation wavelengths corresponding to each cavity length larger than $L_{\min}$. These multiple wavelength addressable cavity lengths translate to multiple FSR which is defined as the wavelength separation between neighboring

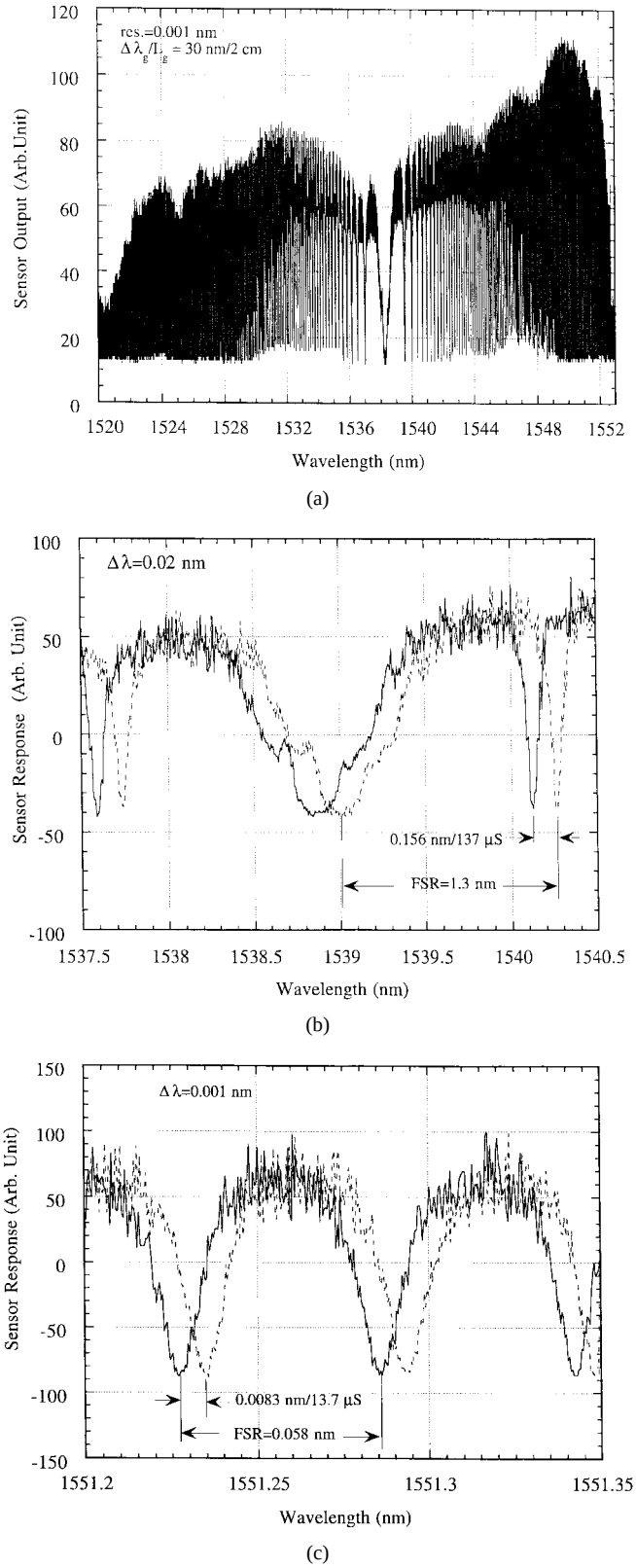

Fig. 3. Spectral responses of the chirped fiber grating FP sensor measured with a wavelength tunable laser scanning (a) from 1520 to 1552 nm with a 0.001-nm step; (b) from 1537.5 to 1540.5 nm with a 0.02-nm step for applied strains of 0 and 137 μStrain; and (c) from 1551.2 to 1551.35 nm with a 0.001-nm step for applied strains of 0 and 13.7 μStrain.

resonance and is approximately equal to $c/2nL_c$, where $c =$ speed of light in vacuum, $n =$ refractive index of glass and

L_c = cavity length. For strain sensing applications with this type of sensor, a range of addressable FSR's implies that a large overall dynamic ranges with high resolution can be achieved with a single sensor head.

Strain sensing using the chirped grating FP fiber cavity was tested by mounting the FP sensor on a metal plate on which a constant strain was applied using a standard four point bending technique [4]. The four-point bending technique allows the calculation of applied strain on the sensor based on the forced deflection of the mounting plate. The spectral response of the chirped grating FP sensor was measured with the tunable laser over the grating passband at wavelength range from 1520 to 1552 nm with resolution as small as 0.001 nm. A series of spectral responses was recorded for different applied strain for scanning wavelengths centered around 1538–1552 nm. Responses at 1552 nm have smaller FSR and higher resolution while response at 1538 nm have larger FSR and lower resolution. Results are presented in the following.

Fig. 3(a) shows the full-wavelength scan (50-min scan time) from 1520 to 1552 nm with wavelength step of 0.001 nm. A range of FSR's has been obtained with the largest FSR centered around 1538 nm and gradual decrease in FSR's toward both the longer and shorter wavelengths. Fig. 3(b) shows the wavelength scan (15 sec scan time) from 1537.5 to 1540.5 nm with wavelength step of 0.02 nm. It shows a measured effective $\mathrm{FSR} = 1.3$ nm ($L_{\mathrm{eff}} = 0.6$ mm) at $\lambda \approx$ 1539 nm and a wavelength shift of 0.156 nm for an applied strain of 137 μStrain or an estimated strain resolution of 15 μStrain for a resolvable wavelength of 0.015 nm. Fig. 3(c) shows the wavelength scan (15-s scan time) from 1551.2 to 1551.35 nm with wavelength step of 0.001 nm. It shows a measured effective FSR = 0.05 nm ($L_{\mathrm{eff}} = 20$ mm) at 1551 nm and a wavelength shift of 0.0083 nm for an applied strain of 13.7 ± 1 μStrain or an estimated strain resolution of 3 ± 1 μStrain for a resolvable wavelength of 0.0018 nm (comparable to the 0.001-nm wavelength resolution of the tunable laser). Therefore, by probing the chirped grating sensor at 1539 and 1551 nm, both large dynamic range and high resolution have been achieved. Note that the defined effective FSR for a chirped grating cavity is different from the conventional FSR for a single FP cavity. An exact analytic expression for the effective FSR is currently being investigated. Low signal to noise in Fig. 3 was due to relatively high detector noise as a result of low optical output power.

Fig. 4 shows the strain-induced spectral shifts and the calculated strain responses from the measured wavelength shifts at various probe wavelengths as a function of the calculated applied strain using the four-point bending model. The tested static strain level extended over 20 dB ranging from 6 to 650 μStrain using the source wavelength scanning approach. The strain resolution of our system is 3 ± 1 μStrain, which is comparable to the strain resolution of 1 μStrain corresponding to the 0.001-nm wavelength resolution of our tunable laser. Higher cavity finesse *may* further increase the strain resolution of our sensor. Fitting the measured strain to the applied strain using a linear curve fitting algorithm shows a linear strain transfer efficiency of 0.8955 with a root-mean-square (rms) error (deviation from linearity) of 0.004 44. The strain induced spectral shift extracted from the data is on the order of 0.001 nm/μStrain which is also comparable to the theoretical limit ($\Delta\lambda/\varepsilon = \zeta\lambda = 1.22 \times 10^{-3}$ nm/μStrain at $\lambda = 1530$ nm) of a FP sensor.

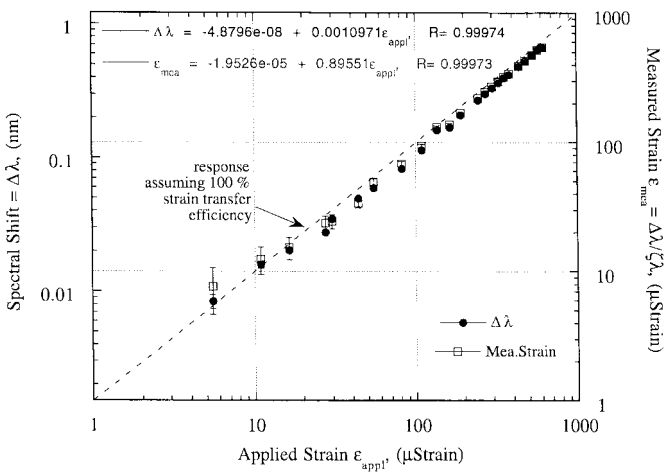

Fig. 4. Strain induced spectral shifts and the corresponding measured strain from the fiber chirped grating FP sensor.

In conclusion, we have demonstrated a fiber chirped grating FP sensor with large dynamic range and high resolution based on the construction of a single sensor head with multiple wavelength addressable FP cavities of different cavity lengths. These FP cavities provide effective free spectral ranges extending from 0.04 to 1.3 nm. Using this chirped grating FP sensor, we measured a static strain sensitivity on the order of 0.001 nm/μStrain (comparable to the theoretical limit of 0.001 22 nm/μStrain) and a dynamic range of 26 dB ranging from 3 ± 1 μStrain to 1300 μStrain. Strain resolution of 3 ± 1 μStrain is limited by the wavelength resolution (0.001 nm) of the tunable source probe (higher resolution is possible with interferometric wavelength detection scheme [5]). This chirped grating FP sensor provides both high resolution and large dynamic range in a single sensor head and thus demonstrates capabilities beyond that of conventional FP sensors.

REFERENCES

[1] J. Sirkis, T. A. Berkoff, R. T. Jones, H. Singh, A. D. Kersey, E. J. Friebele, and M. A. Putnam, "In-line fiber etalon (ILFE) fiber-optic strain sensors," *J. Lightwave Technol.*, vol. 13, pp. 1256–1263, July 1995.

[2] R. A. Atkins, J. H. Gardner, W. N. Gibler, C. E. Lee, M. D. Oakland, M. O. Spears, V. P. Swenson, H. F. Taylor, J. J. McCoy, and G. Beshouri, "Fiber-optic pressure sensors for internal combustion engines," *Appl. Opt.*, vol. 33, no. 7, pp. 1315–1320, Mar. 1994.

[3] G. E. Town, K. Sugden, J. A. R. Williams, I. Bennion, and S. B. Poole, "Wide-band Fabry–Perot-like filters in optical fiber," *IEEE Photon. Technol. Lett.*, vol. 7, pp. 78–80, Jan. 1995.

[4] J. E. Shigley, *Mechanical Engineering Design*, 5th ed. New York: McGraw-Hill, 1989.

[5] A. D. Kersey, T. A. Berkoff, and W. W. Morey, "Fiber-optic grating sensor with drift-compensated high-resolution interferometric wavelength-shift detection," *Opt. Lett.*, vol. 18, no. 1, pp. 72–74, Jan. 1993.